Bismuth-induced embrittlement of copper grain boundaries

GERD DUSCHER[1,2], MATTHEW F. CHISHOLM[1]*, UWE ALBER[3] AND MANFRED RÜHLE[3]

[1]Oak Ridge National Laboratory, Condensed Matter Sciences Division, Oak Ridge, Tennessee 37831-6030, USA
[2]North Carolina State University, Materials Science & Engineering Department, Raleigh, North Carolina 27692, USA
[3]Max-Planck-Institut für Metallforschung, Heisenbergstr. 3, D-70569 Stuttgart, Germany
*e-mail: chisholmmf@ornl.gov

Published online: 22 August 2004; doi:10.1038/nmat1191

Catastrophic brittle fracture of crystalline materials is one of the best documented but most poorly understood fundamental phenomena in materials science. Embrittlement of copper by bismuth is a classic example of this phenomenon. Because brittle fracture in any structural material can involve human tragedy, a better understanding of the mechanisms behind it is of the highest interest. In this study, we use a combination of two state-of-the-art atomic characterization techniques and *ab initio* theoretical materials simulations to investigate the geometric and electronic structure of a copper grain boundary with and without bismuth. Only with this unique combination of methods are we able to observe the actual distribution of bismuth in the boundary and detect changes in the electronic structure caused by the bismuth impurity. We find that the copper atoms that surround the segregated bismuth in the grain boundary become embrittled by taking on a more zinc-like electronic structure.

Losch first proposed the idea that impurity-induced changes to the electronic structure could be responsible for embrittlement in metals[1]. The numerous electronic-structure calculations that followed this seminal work resulted in three proposed mechanisms of embrittlement. The first model proposed that elements that draw charge from the neighbouring metal–metal bonds weaken them and embrittle the materials[1,2]. The second model states that the tendency to embrittlement is determined by whether the impurity is more likely to segregate to a grain boundary or a surface[3,4]. The model suggests that this parameter predicts the relative likelihood of forming a sharp crack (brittle fracture) over a blunt crack (as in a tough material). Using this criterion, the segregation data of Miolinari *et al.*[5] would predict that Bi would not embrittle Cu. The third model states that embrittlement occurs when impurities segregate to the grain boundaries and make the normally non-directional metallic bonds between grains more directional (and less flexible)[1,6]. The directional bonds formed between an impurity and the host metal embrittle the material by impeding stress release. We find that the observed and calculated changes in the electronic structure in the Cu–Bi system are not consistent with any of these models of embrittlement.

Bismuth-doped copper is an ideal system for an atomic-scale investigation of embrittlement. Only two elements are involved, no Cu–Bi intermetallic compounds exist, and there is no evidence that hydrogen (which is always present) embrittles copper. The effect of bismuth segregation on the macroscopic mechanical properties of copper is well documented. Fracture strain[7], fracture stress[8,9] and fatigue life[10] of copper are all adversely affected by the segregation of bismuth to grain boundaries. Studies of bismuth-induced embrittlement of [001] tilt boundaries in copper bicrystals (two crystals tilted around a common [001] axis) have shown that the fracture stress (and strain) can depend strongly on the tilt angle between the two grains[9,11]. Fracture stress capacity was seen to drop rapidly with increased tilt angle, up to ~23°. Between 23° and 67°, the fracture stress capacity was only about a tenth of that obtained for copper single crystals, and the corresponding fracture strain capacity dropped to values near 0%. At any tilt angle in this range, the degree of embrittlement was almost the same. For tilt angles above 67°, the

©2004 Nature Publishing Group

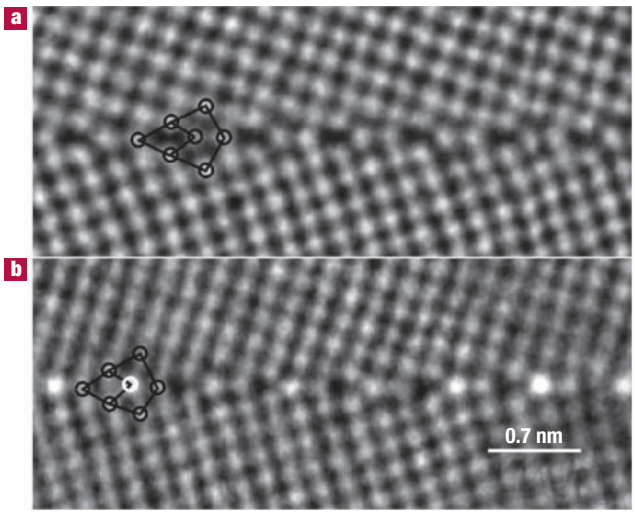

Figure 1 Atomic resolution Z-contrast images of the grain-boundary region of a symmetric 36.8° <001> tilt boundary. a, Pure copper. **b**, Bismuth-doped copper after annealing to produce boundary segregation. Both boundaries consist of a periodic array of an identical structural unit (indicated in image). The bismuth segregation site in **b** is seen to be distinctly bright.

fracture stress capacity increased again[9,11]. These observations are important because it has been predicted that all elemental or random solid solution face-centered-cubic [001] tilt boundaries, such as those in copper, are constructed from a single arrangement of atoms (structural unit)[12]. Because the separation of these structural units for tilt angles between 23° and 67° is always less than 0.9 nm, and our micrographs show that the Bi segregates to the centre of this structural unit, we can calculate the minimum amount of Bi that will embrittle copper. We predict, based on the bicrystal studies[9,11], that a Bi concentration of 8% of the atoms at the grain boundary plane (1.5 Bi atoms per nm^2) is enough to cause catastrophic brittle fractures.

Bismuth is known to induce faceting of copper grain boundaries[13–17]. It has also been shown that the grain-boundary facets disappear if the Bi is removed from the boundary[15]. Sigle *et al.* have demonstrated[17] a correlation between Bi segregation in a copper bicrystal and boundary faceting. They found only a completely faceted boundary exhibited extreme brittle behaviour and suggested that this structural transition is a necessary prerequisite for grain-boundary embrittlement[17]. A key result of their study was to show brittle fracture (actually, boundary faceting) is the result of segregation of a sufficient amount of Bi to the grain boundary, which creates an easy crack path. However, these studies do not show how the segregated bismuth induces embrittlement. In the present study, we have concentrated on the electronic structure changes that result from Bi impurities in Cu. These changes are expected to occur even at single Bi atoms in bulk Cu. But again, brittle fracture will only occur if a sufficient amount of Bi segregates at a two-dimensional defect to form a crack path.

A number of previous studies have found segregation levels of Bi to Cu grain boundaries greater than 1 monolayer. The work of Chang *et al.*[18] and Sigle *et al.*[17] show that Bi enrichment at the boundaries increases for heat treatments in the two-phase (Cu-rich solid + Bi-rich liquid) region of the Cu–Bi phase diagram. It is possible that a different fracture mechanism exists when the Bi enrichment level becomes such that bismuth atoms become nearest neighbours. However, it has been shown in studies using special tilt angle bicrystals[9,11] that very high Bi enrichment levels and the resulting faceting is not necessary to reduce the fracture strain to near zero and the fracture stress to levels nearly a tenth of that of pure copper. The bicrystals investigated in both of these studies and in our study were annealed either within the single-phase region of the Cu–Bi phase diagram or very close to the solidus. These heat treatments result in segregation of Bi to the grain boundaries but at reduced levels compared with those observed when annealing in the grain-boundary wetting region or the two-phase (solid + liquid) region of the Cu–Bi phase diagram of Chang[18].

In this study, we examined symmetric 36.87° [001] tilt grain boundaries. (Details on the growth of the copper bicrystals and bismuth doping have been published previously[16].) The bismuth-doped bicrystal examined in this study was homogenized at 850 °C for 168 hours and had a bulk bismuth content of 25 at. p.p.m., as determined by atomic absorption spectroscopy. Subsequently, the bicrystal was annealed at 700 °C for 240 hours to produce grain-boundary segregation[16]. Quantitative energy-dispersive spectroscopy (EDS) showed Bi present with an areal density of 2.9 Bi atom per nm^2 in the grain-boundary region[16] (nearly twice as much as what we have predicted to be necessary to embrittle copper based on the work in refs 9 and 11).

The Z-contrast imaging technique was used to determine the structure of the grain boundary and to directly observe the positions of the bismuth impurities in the boundary. A Z-contrast image is formed by scanning a focused electron probe over the specimen and collecting scattered electrons with a high-angle annular detector. The unique scanning transmission electron microscope (VG HB 603 U) at the Oak Ridge National Laboratory produced at the time of these experiments an electron probe with a diameter of 0.12 nm, much less than the atomic distances in copper. High-angle electron scattering allows images to be obtained in which the intensity is proportional to the square of the atomic number, Z; thus, heavier atoms appear brighter in the images[19]. The images show stacks of atoms (atomic columns) as bright spots. These images allow straightforward detection of heavy impurities (such as Bi) segregated to grain boundaries. Figure 1 compares Z-contrast images of the non-doped (a) and the Bi-doped (b) boundaries. In this [001] projection, the atomic columns in the copper grains form a square grid of bright dots separated by 0.18 nm. The boundary in both samples consists of a periodic array of a defect structural unit (as indicated in Fig. 1). The structural unit contains four under-coordinated atoms. One of the four under-coordinated atomic columns in each structural unit of the bismuth-doped boundary is seen to be distinctly bright. The extra intensity is consistent with the presence of an impurity with an atomic number much greater than copper, in this case Bi.

The images make it clear that this grain-boundary configuration is little affected by the presence of bismuth. No new phases are formed and no drastic atomic rearrangements occur as the result of bismuth segregation to this boundary. Bismuth simply substitutes for Cu on a preferred atomic site in the boundary core. Previous atomistic simulations of this boundary have indicated that this site is the preferred segregation point for impurities larger than Cu, such as Sb (ref. 20), Bi (ref. 21) and Ag (ref. 22). These larger impurities all prefer the boundary site with the largest space. Because there is no change in symmetry or bond length at the grain boundary, the embrittlement cannot be explained simply as due to changes in the atomic configuration.

The electronic structure of the grain-boundary region was measured directly with electron energy loss spectroscopy (EELS). The Z-contrast images and EELS spectra can be collected simultaneously, thus ensuring the spectra are obtained from the area of interest. To determine the grain-boundary component of the absorption spectra, we used the spatial difference technique. In this technique, a spectrum is taken from a small area containing the boundary. This area also contains bulk-like copper, so reference spectra from the adjacent grains are recorded, normalized and subtracted from the boundary spectrum.

The spatial difference technique can be misleading if the analysed volume is large relative to the feature of interest. Small changes are

©2004 Nature Publishing Group

rendered barely detectable as the fraction of boundary atoms within the analysed volume is reduced to <10%. We were able to reproduce published results when using the 3 nm × 4 nm analysis area described in earlier studies[23–25]. Only by using 1.5 nm × 2 nm analysis volumes, made possible by the single-electron sensitivity of our charge-coupled device detector, were we able to detect and interpret changes to the near-edge structure more accurately.

EELS probes the local electronic structure through core-loss absorption (excitation of a core–shell electron into the conduction band). Figure 2 shows spectra with the Cu-L_3 absorption edge (excitation from 2*p* core–shell to the conduction band) at the non-doped and doped grain boundary and reference spectra from the adjacent grains. The thicknesses of the analysed regions were found to be approximately a third of the mean free path for inelastic scattering as determined from low-loss spectra. Spectra from the Cu-L_3 edge, recorded from a region at the non-doped boundary and well away from the boundary, are shown in Fig. 2a. The spectra in Fig. 2a from the non-doped boundary and the adjacent crystal are nearly indistinguishable. This shows that there is very little intrinsic effect on the electronic structure from the non-doped grain boundary. However, Fig. 2b shows that the Cu-L_3 edge is affected by the presence of bismuth in the boundary. The three small peaks superimposed on the step-like edge are considerably reduced in the spectrum from the doped boundary. This observation can be analysed as a change in bonding of the copper atoms at the doped grain boundary.

In a copper crystal, the 3*d* states lie close to the top of the valance band and mix with the 4*s* states. The first Cu-L_3 peak is due to the onset of the absorption edge. The two other peaks in the Cu-L_3 edge are a result of this *s*–*d* state mixing (hybridization). More precisely, the second and third peaks (~4 eV and 7 eV above the Fermi level) are associated with van Hove singularities in the copper free-electron-like states at the *L* and *X* points[26]. However, the Cu-L_3 absorption edge is predominately due to states with *d* character; thus, these two peaks that originate from *s*-bands are seen due to hybridization with *d*-states. The most significant changes induced by the Bi are the suppression of the onset peak and the two peaks associated with the van Hove singularities. This would suggest a reduction of the density of *d*-like states at the Fermi level and reduced hybridization between *d* and *s* states for the copper atoms that surround the bismuth. Both of these results also imply reduced covalent (directional) bonding among Cu 3*d* electrons in the boundary region.

Unlike bonds in other metals, the bonds in noble metals are strengthened by directionality, which is induced by *s*–*d* hybridization. This increased bond strength was described through calculation of noble metal stacking fault energies that decrease with decreased *s*–*d* hybridization[27]. Our EELS results suggest that embrittlement of Cu by Bi occurs with reduced *s*–*d* hybridization and, thus, reduced directional bonding of the copper atoms surrounding the bismuth impurity. This contradicts the third embrittlement mechanism described in the introduction of this article in which an impurity embrittles by increasing bond directionality.

The choice of a small period tilt boundary makes it possible to combine high-resolution imaging with first principles calculations. We believe this benefit outweighs the fact that it is a special boundary type, but we certainly admit the observed and tested structures do not cover all possible boundary arrangements. The calculations were performed using density functional theory with local density approximation. The Z-contrast images provided a well-defined starting model for the materials simulations. These calculations yield the lowest-energy atomic configuration of the grain-boundary region, its associated electron distribution (charge density) and site- and momentum-resolved density of states. The calculated structure is shown in Fig. 3a. Very few differences are seen in the calculated atomic configuration of the grain boundary with and without bismuth. The most significant change is a very slight expansion of the boundary width, defined as the change in separation of twin-related

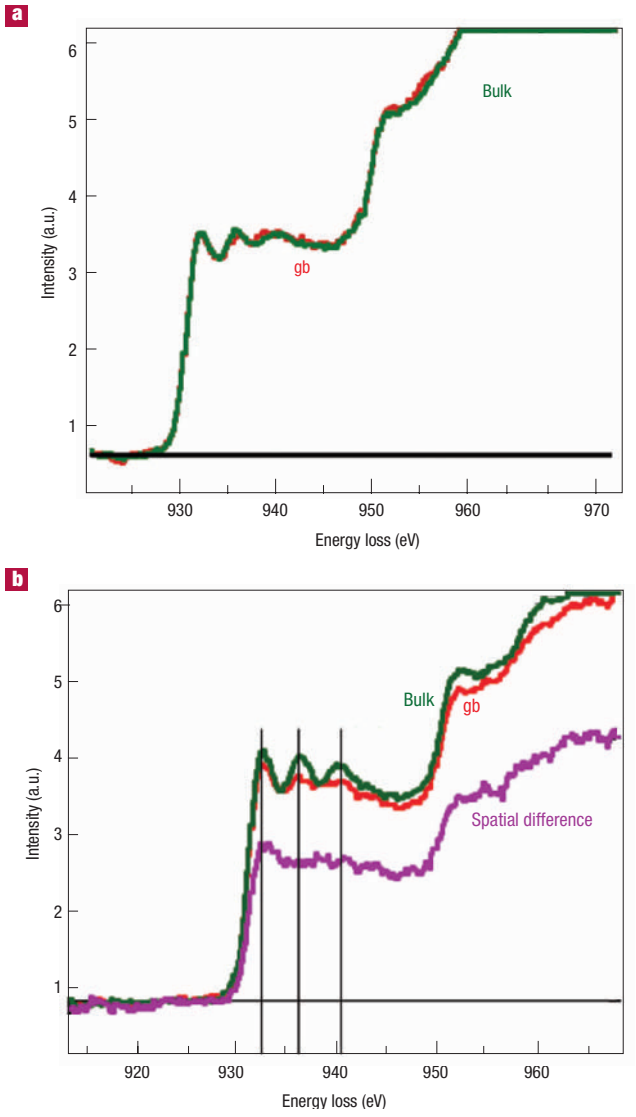

Figure 2 Experimental Cu-L_3 near-edge structure from the grain boundary and the adjacent grains. a, The non-doped bicrystal. **b**, The bismuth-doped bicrystal. The EELS spectra in **a** from the clean boundary (gb) and copper crystal (bulk) show no significant differences, indicating very little change in *s*–*d* hybridization at this bismuth-free boundary. The spectra from the boundary containing bismuth (**b**) show a suppression of the two peaks in the Cu-L_3 edge, at 4 eV and 7 eV above the onset peak.

copper atoms on either side of the boundary (differences range from 7 pm to 10 pm).

An impurity of a larger size is expected to segregate to sites where bonds are already strained. It has been proposed that embrittlement is due to additional straining of these weakened bonds. Although this misfit is important for the segregation of bismuth, there is no evidence that strain alone can embrittle copper grain boundaries, because we found no dramatic changes in bond length with or without bismuth. As mentioned, antimony, bismuth and silver segregate to copper grain boundaries and are similarly sized but silver does not embrittle copper, suggesting the effect is not simply mechanical.

The relaxed structures of the supercells were used to calculate the site and momentum projected density of states (DOS) and from that

©2004 Nature Publishing Group

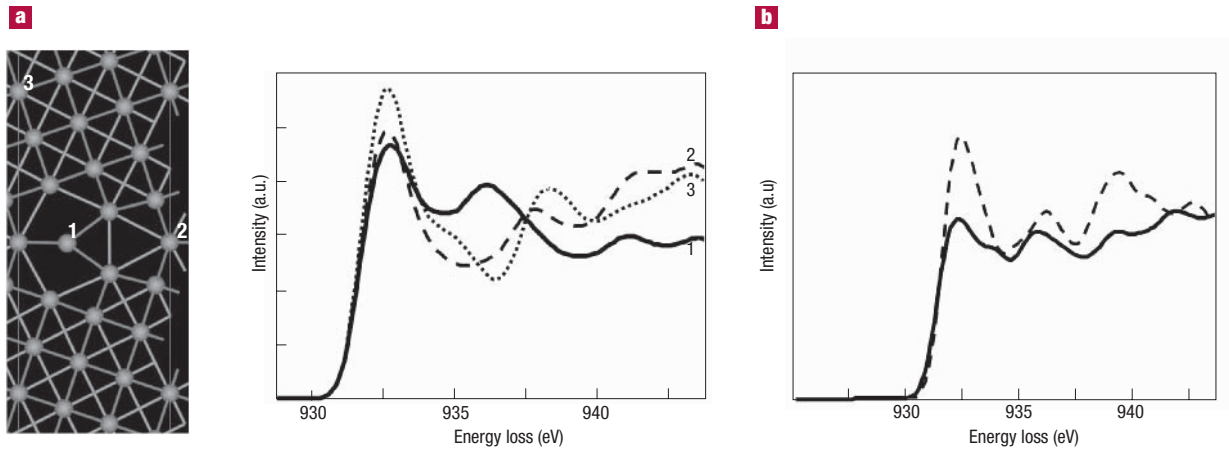

Figure 3 Calculated Cu-L_3 near-edge structure from the boundary region. **a**, Non-doped boundary supercell. **b**, Bismuth-doped boundary supercell. The ELNES spectra in **a** show that there is only one site (site 1, the impurity segregation site) that is significantly different from bulk copper. The calculated spectra in **b** are from the nine sites that surround the bismuth impurity in the boundary (solid line) and from undistorted Cu sites between the boundaries (dashed line).

the energy-loss near-edge structure (ELNES) of the Cu-L_3 edge. To reproduce the experimental ELNES in bulk Cu, a 64 atom unit cell was found to be necessary with a k-point sampling of 8 × 8 × 8. Approximately the same k-point density and number of atoms as in bulk calculation cells was used in the supercells with grain boundaries. The Z+1 approximation, used successfully in semiconductor and ceramic materials, was also tested and found to produce poor agreement with experiment. This had been seen in previously published calculations and is to be expected from a metal due to more effective screening of the core hole[28,29].

The three features seen in the experimental L_3 edges are reproduced in the ELNES simulations shown in Fig. 3. The site and angular momentum projected DOS are convoluted with a gaussion of 0.8 eV to represent the experimental resolution. Then 95% of *d*- and 5% of *s*-projected DOS were summed. (These transition probabilities were calculated with an all-electron augmented plane-wave calculation of bulk copper, using WIEN 97). Our ELNES simulations show that at the pure Cu grain boundary there is only one atomic site (the site to which Bi segregates in the middle of the pentagonal arrangement on the boundary) with a significantly different ELNES. As seen in Fig. 3a, even the other site on the boundary plane has a calculated ELNES very similar to that from a bulk Cu site. This finding explains why we do not detect experimentally any change of the ELNES at the pure Cu grain boundary. The mechanical effect of strained bonds caused by segregation of a large impurity was also examined by replacing the Bi atoms in the relaxed supercell with Cu (without further relaxation). The ELNES simulations of this supercell structure (not shown) yield only a slight difference from the pure Cu grain boundary. This indicates that it is not strain alone that is responsible for the observed changes in the electronic structure. Bismuth segregation results in clear changes in the calculated electronic structure and a more extensive boundary-affected region. Figure 3b shows that the calculated ELNES from atomic (Cu) sites up to 0.5 nm from the grain boundary (9 atomic sites in this boundary) are significantly different from those of bulk copper. We see that the Cu-L_3 edge at the Bi-doped grain boundary shows a reduction of all three maxima, compared with the calculated Cu bulk ELNES as was seen experimentally. This further strengthens the interpretation of our experimental results that there are a reduced number of unoccupied *d* holes at or above the Fermi level and reduced hybridization between *d* and *s* states for the copper atoms that surround the Bi impurities. The calculated and experimental spectra are in good agreement.

These conclusions can be tested by analysing the partial density of states of the valence-band. Figure 4 shows that the filled *d* bands of Cu in the boundary region are narrowed and sharpened relative to the bulk DOS. This is consistent with a more closed *d* shell. The *sp*-DOS has less structure in the region of these *d* bands, which indicates reduced hybridization. At the Fermi level, we see that the number of *d* valence states is reduced at the Bi-doped grain boundary. The valence band DOS, therefore, yields the same interpretation as the DOS of the conduction band, which was probed experimentally with EELS.

The calculated electron charge density reveals another dramatic effect (Fig. 5). Figure 5b is a slice of the charge-density difference, obtained by subtracting the charge density of a reference system (a supercell with the same atomic positions but with Cu instead of Bi) from the charge density for the lowest-energy Bi-doped structure. This {001} slice is taken from the plane between Bi impurities that contains a Bi impurity's nearest Cu neighbours. The segregation of Bi results in an electron cloud (the coloured areas in Fig. 5b) that extends out beyond the surrounding copper sites. Even the second and third nearest neighbours are affected by this enhanced electron density, originating from the metallic bonding of Bi to Cu. The calculated charge-density difference also reveals that Bi induces a slight reduction in the directionality of bonding between Cu atoms. See the Supplementary Information for further discussion and an additional figure. The reduced bond directionality contradicts the third embrittlement mechanism described in the introduction of this article.

The enhanced electron density at the copper sites that surround the Bi impurity means that electrons further fill the usually half-filled *s* bands of copper. This *s*-band filling can be described as a population of antibonding states, which reduces the bond strength between the copper atoms. To further explore the origin of this effect and to validate our calculations, we replaced the Bi with silver atoms in our calculations. Figure 5c shows that the charge-density difference plot is strikingly different from the bismuth plot. The electron density of the silver remains localized at the impurity location, only slightly affecting the immediate Cu neighbours.

We have demonstrated that the Cu–Bi system exhibits a class of behaviour not predicted by current embrittlement models.

©2004 Nature Publishing Group

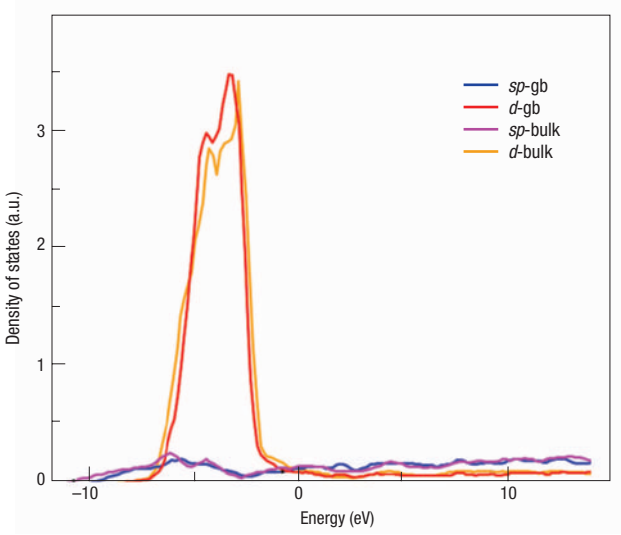

Figure 4 Comparison of the DOS between the Bi-doped Cu grain boundary (7 nearest neighbours of Bi) and bulk Cu. Shown are the calculated *s*+*p* and *d* partial density of states of the valence and conduction band. The Fermi level is at zero eV.

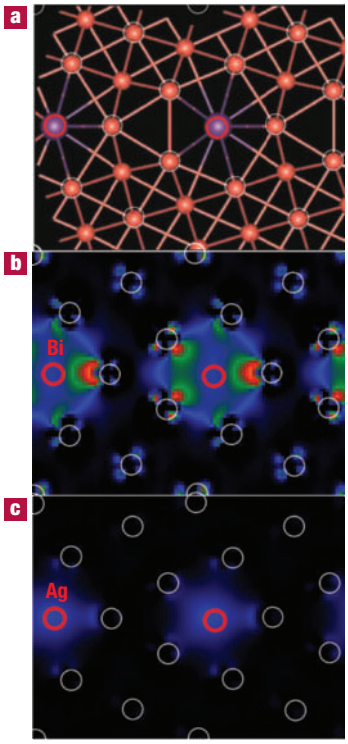

Figure 5 Calculated charge density from copper grain-boundary region. a, The calculated grain-boundary structure. The red circle indicates the impurity segregation site. **b**,**c**, The calculated charge-density-difference plot ([001] slice centred on the plane above the impurity) is shown for Bi-doped (**b**), and silver-doped (**c**) boundary region. The brighter colours indicate higher electron density; the yellow regions contain up to 0.06, green up to 0.04, red up to 0.02 and blue up to 0.01 electrons per pixel.

Essentially, Cu in the boundary becomes embrittled by taking on a zinc-like electronic structure. The copper atoms surrounding the segregated Bi exhibit a closed 3*d* shell, reduced *s*–*d* hybridization and most importantly an *s* band that is more than half full. None of these effects are a good thing for fracture toughness. This effect is expected to be independent of the atomic arrangement at the grain boundary and thus it is applicable to any Bi-doped grain boundary in Cu.

It is certainly possible that a different fracture mechanism exists when the Bi impurity level is such that Bi atoms become nearest neighbours. The electronic structure changes we describe may no longer dominate the fracture mechanism when there are multiple layers of segregated impurities. We have not yet investigated that possibility. The electronic structure of these boundaries could and should be evaluated once their geometric structure has been determined.

METHODS

The calculations were done using a supercell with 60 atoms and two boundaries in which the atoms are represented by ultra-soft pseudopotentials, and a plane-wave basis set. Density functional theory with the local density approximation as incorporated in the Vienna Ab-initio Simulation Package (VASP) was used to relax this supercell and obtain the equilibrium charge densities[30].

Received 4 February 2004; accepted 8 June 2004; published 22 August 2004.

References

1. Losch, W. A new model of grain boundary failure in temper embrittled steel. *Acta Metall.* **27,** 1885–1892 (1979).
2. Messmer, R. P. & Briant, C. L. The role of chemical bonding in grain boundary embrittlement. *Acta Metall.* **30,** 457–467 (1982).
3. Rice, J. R. & Wang, J.-S. Embrittlement of interfaces by solute segregation. *Mater. Sci. Eng. A* **107,** 23–40 (1989).
4. Wu, R., Freeman, A. J. & Olson, G. B. First principles determination of the effects of phosphorus and boron on iron grain boundary cohesion. *Science* **265,** 376–380 (1994).
5. Miolinari, C. & Joud, J. C. in *Physical Chemistry of the Solid State: Applications to Metals and their Compounds* (ed. Lacombe, P.) 151–163 (Elsevier, Amsterdam, 1984).
6. Haydock, R. The mobility of bonds at metal surfaces. *J. Phys. C* **14,** 3807–3816 (1981).
7. Hondros, E. D. & McLean, D. Cohesion margin of copper. *Phil. Mag.* **29,** 771–795 (1974).
8. Russell, J. D. & Winter, A. T. Orientation effects in embrittlement of copper bicrystals by bismuth. *Scripta metall.* **19,** 575–579 (1985).
9. Li, G. H. & Zhang, L. D. Relationship between misorientation and bismuth induced embrittlement of [001] tilt boundary in copper bicrystal. *Scripta metall.* **32,** 1335–1340 (1995).
10. Chikwembani, S. & Weertman, J. Fatigue and fracture of copper-bismuth bicrystals. *Scripta Metall.* **19,** 1499–1502 (1985).
11. Miura, H., Nakata, H., Sakai, T., Kato, M. & Mori, T. Temperature dependence of embrittlement of Cu[001] symmetrical tilt boundaries induced by Bi segregation. *J. Jpn Inst. Metals* **58,** 477–482 (1994).
12. Smith, D. A., Vitek, V. & Pond, R. C. Computer simulation of symmetrical high angle boundaries in aluminium. *Acta metall.* **25,** 475–483 (1977).
13. Voce, E. & Hallowes, A. P. C. The mechanism of the embrittlement of deoxidized copper by bismuth. *J. Inst. Metals* **74,** 323–376 (1947).
14. Donald, A. M. & Brown, L. M. Grain boundary faceting in Cu-Bi alloys. *Acta Metall.* **27,** 59–66 (1979).
15. Ference, T. G. & Balluffi, R. W. Observation of a reversible grain boundary faceting transition induced by changes of composition. *Scripta Metall.* **22,** 1929–1934 (1988).
16. Alber, U., Müllejans, H. & Rühle, M. Bismuth segregation at copper grain boundaries. *Acta Mater.* **47,** 4047–4060 (1999).
17. Sigle, W., Chang, L.-S. & Gust, W. On the correlation between grain-boundary segregation, faceting and embrittlement in Bi-doped Cu. *Phil. Mag. A* **82,** 1595–1608 (2002).
18. Chang, L.-S., Rabkin, E., Straumal, B. B., Baretzky, B. & Gust, W. Thermodynamic aspects of the grain boundary segregation in Cu(Bi) alloys. *Acta Mater.* **47,** 4041–4046 (1999).
19. Jesson, D. E. & Pennycook, S. J. Incoherent imaging of thin specimens using coherently scattered electrons. *Proc. R. Soc. Lond. A* **441** 261–281 (1993).
20. Chang, H. K., Weidman, R. S. & Lee, J. K. An atomistic study of grain boundary segregation and cracking. *Surf. Sci.* **144,** 224–252 (1984).
21. Vitek, V., Ackland, G. J., Menyhard, M. & Yan, M. in *Interfaces: Structure and Properties* e(d. S. Ranganathan) 3–19 (Trans Tech, Aedemannsdorf, Switzerland, 1993).
22. Menyard, M., Yan, M. & Vitek, V. Atomistic vs. phenomenological approaches to grain boundary segregation: Computer modeling of Cu-Ag alloys. *Acta Metall.* **42,** 2783–2796 (1994).
23. Bruley, J., Keast, V. J. & Williams, D. B., Measurement of the localized electronic structure associated with bismuth segregation to copper grain boundaries. *J. Phys. D* **29,** 1730–1739 (1996).
24. Keast, V. J., Bruley, J., Rez. P., MacLaren, J. M. & Williams D. B. Chemistry and bonding changes associated with the segregation of Bi to grain boundaries in Cu. *Acta Mater.* **46,** 481–490 (1998).
25. Bruley, J., Keast, V. J. & Williams, D. B. An EELS study of segregation-induced grain boundary embrittlement of copper. *Acta Mater.* **47,** 4009–4017 (1999).

©2004 Nature Publishing Group

26. Ebert, H., Stohr, J., Parkin, S. S. P., Samant, M. & Nilsson, A. L-edge x-ray absorption in fcc and bcc Cu metal: Comparison of experimental and first-principles theoretical results. *Phys. Rev. B* **53,** 16067–16073 (1996).
27. Schweizer, S., Elsasser, C., Hummler, K. & Fahnle, M. Ab initio calculation of stacking-fault energies in noble metals. *Phys. Rev. B* **46,** 14270–14273 (1992).
28. Luitz, J. *et al.* Partial core hole screening in the Cu L3 edge. *Eur. Phys. J. B* **21,** 363–367 (2001).
29. Hebert, C., Luitz, J. & Schattschneider, P. Improvement of energy loss near edge structure calculation using Wein2k. *Micron* **34,** 219–225 (2003).
30. Kresse, G. & Furthmüller, J. Efficient iterative schemes for *ab initio* total-energy calculations using a plane-wave basis set. *Phys. Rev. B* **54,** 11169–11186 (1996).

Acknowledgements

This research was sponsored by the Office of Basic Energy Sciences, US Department of Energy at Oak Ridge National Laboratory under contract DE-AC05-00OR22725 with UT-Battelle and by the Deutsche Forschungsgemeinschaft under contract HO 708/15-1.
Correspondence and requests for materials should be addressed to M.F.C.
Supplementary Information accompanies the paper on www.nature.com/naturematerials

Competing financial interests

The authors declare that they have no competing financial interests.

©2004 Nature Publishing Group